



Preparation and characterization of nylon 11/organoclay nanocomposites

Tianxi Liu*, Kian Ping Lim, Wuiwui Chauhari Tjiu, K.P. Pramoda, Zhi-Kuan Chen*

Institute of Materials Research and Engineering, 3 Research Link, Singapore, Singapore 117602

Received 9 December 2002; received in revised form 4 March 2003; accepted 7 March 2003

Abstract

Nylon 11/organoclay nanocomposites have been successfully prepared by melt-compounding. X-ray diffraction and transmission electron microscopy indicate the formation of the exfoliated nanocomposites at low clay concentrations (less than 4 wt%) and a mixture of exfoliated and intercalated nanocomposites at higher clay contents. Thermogravimetric and dynamic mechanical analyses as well as tensile tests show that the degree of dispersion of nanoclay within polymer matrix plays a vital role in property improvement. The thermal stability and mechanical properties of the exfoliated nylon 11/clay nanocomposites (containing lower clay concentrations) are superior to those of the intercalated ones (with higher clay contents), due to the finer dispersion of organoclay among the matrix.

© 2003 Elsevier Science Ltd. All rights reserved.

Keywords: Nylon 11; Clay; Nanocomposites

1. Introduction

Polymer/clay nanocomposites—a new class of reinforced plastics formed by dispersing nano-sized clay particles throughout a polymer matrix—have received much attention in both scientific and industrial arenas due to their enhanced mechanical and barrier properties as well as flame resistance [1–5]. Generally, three methods for the formation of polymer/clay nanocomposites are mainly used: (1) Intercalation of monomers followed by in situ polymerization; (2) Direct intercalation of polymer chains from solution; (3) Polymer melt intercalation. Each of these methods has its advantages and disadvantages. For example, the direct melt intercalation into clay layers is a preferred process for the formation of hybrid materials not only with respect to environmental issues (solvent free), but also due to the ease of fabrication for its promising commercial applications [6]. Usually, the dispersion of clay particles in a polymer matrix results in the formation of three types of composite materials. The first type is conventional phase separated composites in which the polymer and the inorganic host remain immiscible resulting in poor mechanical properties of the composite material. The second type is intercalated polymer-clay nanocomposites, which are

formed by the insertion of one or more molecular chains of polymer into the interlayer or gallery space. The last type is exfoliated or delaminated polymer-clay nanocomposites, which are formed when the clay nanolayers are individually dispersed in the continuous polymer matrix. Exfoliated polymer-clay nanocomposites are especially desirable for improved properties because of the large aspect ratio and homogeneous dispersion of clay and huge interfacial area (and consequently strong interaction) between polymer chains and clay nanolayers. Although extensive efforts have been devoted to the preparation and characterization of polymer/clay nanocomposites, the mechanisms responsible for the improvements in physical and mechanical properties have not yet been fully identified.

The pioneering work on nylon 6-based clay nanocomposites was first developed by Toyota research group [7–10]. Many investigations on preparation, characterization and mechanical property [11–13], on the influences of crystalline structure and morphology of nylon 6 due to clay addition [14–18], on thermal degradation [19] and rheology [20] have since been followed. Nylon 11 is an important commercial polyamide with excellent piezoelectricity and mechanical properties and used in a large range of industrial fields from automotive to offshore applications. It has multiple crystal forms (polymorphism), which is greatly dependent on the thermal history and closely related to the piezoelectric and ferroelectric responses [21,22]. To the best of our knowledge, no study on nylon 11/clay

* Corresponding authors. Tel.: +65-6874-8594; fax: +65-6774-4657.

E-mail addresses: liu-tx@imre.a-star.edu.sg (T. Liu),
zk-chen@imre.a-star.edu.sg (Z.K. Chen).

nanocomposites has been reported yet. In this study, a series of nylon 11 nanocomposites with different degrees of clay exfoliation and intercalation has been prepared by direct melt-compounding and their nanoscale morphologies as well as thermal and mechanical properties have been characterized.

2. Experimental part

2.1. Materials and sample preparation

The material used in this study was nylon 11 (polyamide 11, PA11) pellets (Rilsan Besno TL[®], Atofina). The unmodified pristine clay and organically modified clay (organoclay: Nanomer[®] I.34TCN) were supplied by Nanocor Inc. The supplier does not provide the detailed information on the chemical structures of the nanomer (such as modifier type, cation exchange capacity (CEC)). Since polyamides are very easy to absorb moisture, prior to compounding all the samples were dried in vacuum oven at 80 °C for 24 h in order to remove the absorbed water. Otherwise, it is difficult to obtain bubble-free specimens by compression molding. A wide range of nylon 11/organoclay nanocomposites containing 0, 1, 2, 4 and 8 wt% organoclay was prepared via melt-compounding method using a Brabender twin-screw extruder at 220 °C with a screw speed of 80 rpm. The as-received nylon 11 pellets and the obtained nanocomposites were placed in a mold that was positioned between two steel plates covered with aluminium foil. Film samples (with thicknesses of 0.5 and 1 mm) were prepared by compression molding in a press at a temperature of 220 °C and a pressure of 150 bar, followed by a quick quenching in an ice/water bath to get amorphous sheets.

2.2. X-ray diffraction and transmission electron microscopy

X-ray diffraction (XRD) patterns of the as-extruded samples were recorded using a Bruker GADDS diffractometer with area detector operating under a voltage of 40 kV and a current of 40 mA using Cu K α radiation ($\lambda = 0.15418$ nm). Ultrathin sections (with thickness of ca. 70 nm) for transmission electron microscopy (TEM) observations were cut from as-extruded nanocomposite pellets under cryogenic conditions using a Leica ultramicrotome with a diamond knife. Due to a large difference in electron density between clay and polymer matrix, no selective staining is required. The TEM micrographs were taken using Philips CM300-FEG transmission electron microscope under an accelerated voltage of 150 kV.

2.3. TGA and DMA measurements

Thermogravimetric analysis (TGA) was performed under both air and nitrogen flows from 50 to 800 °C at a heating rate of 20 °C/min by using a Perkin–Elmer TGA 7.

Dynamic mechanical analysis (DMA) was performed on the samples of $30 \times 10 \times 0.5$ mm³ in size using a dynamic mechanical analyzer from TA Instruments under tension film mode in a temperature range of -100 – 150 °C at a frequency of 1 Hz and heating rate of 3 °C/min.

2.4. Mechanical testing

The obtained amorphous films were finally punched into dog-bone sheets with dimension of $63.5 \times 9.53 \times 3.18$ mm³ (Die ASTM D-638 Type V) using a CEASt hollow die punch (model 6051). The tensile tests were carried out using an Instron machine (Model 5567) at room temperature. The gauge length was set as 30 mm and the crosshead speed was set at 5 mm/min. An extensometer (Model 2630-105) was used to accurately determine the elastic modulus from the initial part (at deformation of 0.1%) of stress–strain curves. Property values reported here represent an average of the results for tests run on at least six specimens. Prior to testing, all specimens were dried in a vacuum oven at 80 °C for 12 h.

3. Results and discussion

3.1. Nanostructure and morphology

The clay dispersion within nylon 11 matrix has been characterized by both XRD and TEM. Fig. 1 illustrates the XRD patterns for neat nylon 11 and its organoclay nanocomposites with different clay concentrations. The XRD patterns for the pristine clay and organically modified

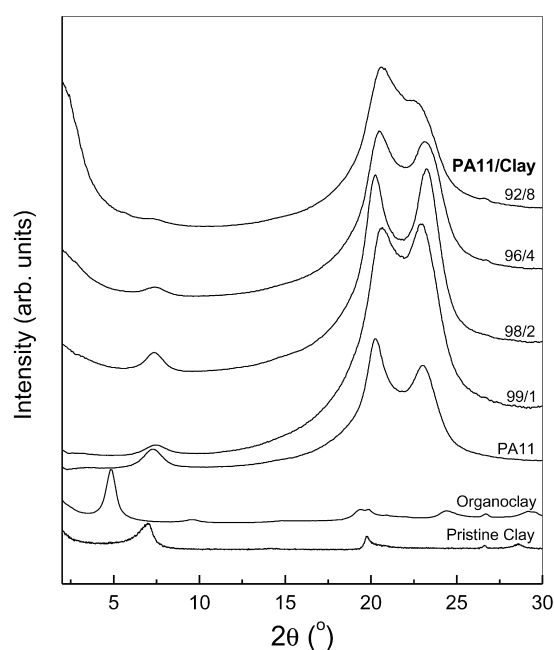


Fig. 1. XRD patterns of the pristine and modified clay, neat PA11 and its organoclay nanocomposites.

clay (organoclay) are also shown for comparison. The XRD pattern of the pristine clay mineral shows a reflection peak at about $2\theta = 7.0^\circ$, corresponding to a basal spacing of 1.4 nm. After modification by organic surfactant, for organoclay the reflection peak of the basal plane dramatically shifts to $2\theta = 3.9^\circ$ with a d -spacing of 2.5 nm, indicating that a swollen and intercalated structure is formed in organoclay after surface modification. As a result, after incorporating with nylon 11 by melt-compounding the basal plane of organoclay disappears in the XRD patterns for the obtained nanocomposites with different clay loading levels up to 8 wt%. The absence of basal plane peaks indicates the delamination and dispersion of the clay nanolayers within the PA11 matrix, i.e. the formation of an exfoliated nanostructure. Note that the three main reflection peaks at $2\theta = 7.2, 20.2, 23.0^\circ$ correspond to (001), (100) and (010/110) planes of the α -form crystals for nylon 11, respectively [23]. In contrast to nylon 6/clay nanocomposites [14–18], the addition of clay does not change the crystalline structures of nylon 11 (when at low temperatures, such as lower than 100 °C), as also reported by Kuchta and co-workers [24]. This means that the PA11/clay nanocomposites still crystallize in their stable triclinic α -form. Interestingly, our preliminary results show that there is an α -form to γ -form crystal transition upon deformation for PA11/clay nanocomposites. The detailed work on the effect of clay addition on the crystalline structure and morphology of nylon 11 is still in progress.

It is worthy noting that in spite of the absence of the basal plane, a broad shoulder in the small-angle region is usually observed in XRD patterns for the obtained nanocomposites with high clay loading (e.g. 8 wt%), probably indicating the formation of partially exfoliated/partially intercalated nanostructures. Hence, it seems reasonable that Kojima et al. used the peak intensity together with the interlayer spacing (i.e. peak position) to characterize the relative proportion of exfoliated and intercalated species with the nanofiller content [25]. Here, from the XRD patterns of PA11/clay nanocomposites, it is likely that the exfoliated structure is the dominant population when the clay concentration is below 4 wt%; and above it, the intercalated hybrid gradually dominates; and between the two extremes (for clay loading of ca. 4 wt%), the exfoliated structure with partially structural ordering is probably formed [26]. These speculations have been further confirmed by TEM observations as illustrated in Fig. 2. Two TEM images (A) and (B) show typical but different clay dispersions for PA11 nanocomposites containing organoclay of 2 and 8 wt%, respectively. It can be seen that the clay platelets (separated dark lines) with thickness of ca. 1 nm are homogeneously dispersed in the polymer matrix in both cases. Clearly, the former (at low clay loading, 2 wt%) is a typical characteristic of disordered and exfoliated clay nanostructure; whereas the latter (at high clay loading, 8 wt%) is typically ordered intercalated nanoclay morphology. Close inspection of the well-dispersed clay domains in Fig. 2(B) reveals

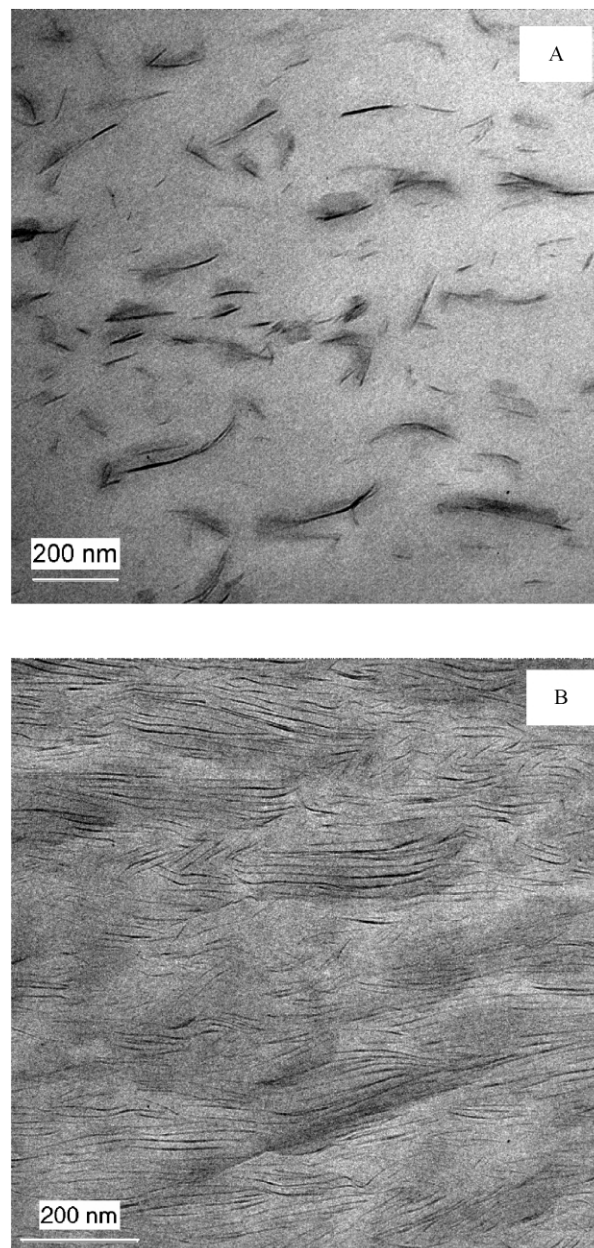


Fig. 2. Bright field TEM images of PA11/clay nanocomposite. PA11/clay: 98/2 (A) and 92/8 (B).

consistent nanolayer spacings of about 10 nm or more, which explains why no diffraction peak is observed on its XRD pattern (see Fig. 1). However, the ordered intercalated structure of nanolayer still maintains for the nanocomposite with high clay loading.

It should also be noted that in practice it is difficult to get fully exfoliated (or fully intercalated) polymer/clay nanocomposites at higher clay loadings, especially by melt intercalation approach. The relative fraction of intercalation/exfoliation usually increases with increasing the clay concentration. This is illustrated by a smooth shoulder with a gradual increase in the diffraction intensity at low angle in the XRD pattern, probably suggesting a complex structure

with partial exfoliation along with partial intercalation. At high clay loading (e.g. 8 wt%), clay agglomeration is usually inevitable to some extent. In addition, diverse nanoscale morphologies of clay are usually observed by TEM. Therefore, although it is common practice to classify a nanocomposite as fully exfoliated from the absence of (001) basal reflections, the TEM images shown here reveal a more complex situation. Actually, the coexistence of exfoliated and intercalated nanostructures is frequently observed in a number of thermoplastic and thermoset polymer/clay nano-systems [26–29]. This complexity of organoclay morphologies among polymer matrices may be definitely reflected by the changes in thermal and mechanical properties of the final products.

3.2. Thermal stability and dynamic mechanical behavior

The thermal stability of neat PA11 and the nanocomposites has been investigated by TGA under both nitrogen and air flows (Fig. 3). Only the TGA traces in nitrogen are shown here. The insert (bottom left) clearly shows that the onset (at weight loss of 5%) of decomposition temperature is significantly improved by about 20 °C at low nanofiller concentrations (less than 4 wt%) and quickly levels off, especially in air flow. In contrast, at high clay content (such as 8 wt%), the (intercalated) nanocomposite degrades at temperature 5–10 °C inferior to the degradation of the pure unfilled PA11 matrix. However, all the TGA traces show a shift of the weight loss towards higher temperatures, for example, with a stabilization as high as ca. 8 °C at 50%

weight loss for PA11/clay (92/8) nanocomposites. Therefore, these TGA results are very informative. It is usually well accepted that the improved thermal stability for polymer/clay nanocomposites is mainly due to the formation of char which hinders the out-diffusion of the volatile decomposition products, as a direct result of the decrease in permeability, usually observed in exfoliated nanocomposites [30]. For the studied nylon 11/clay system, it seems that (1) the enhanced thermal stability is only achieved at quite low loading level, thus making the obtained nanocomposites cheaper, lighter and easier to process than the conventional microcomposites, (2) the improvement in thermal stability is much more significant for the exfoliated nanocomposites than that for the intercalated ones. Optimal thermal stabilization is achieved at clay concentration of ca. 2–4 wt%, as also observed in ethylene-vinyl acetate (EVA) copolymer-based clay nanocomposites [30]. Below this value no dramatic improvement on thermal stability is observed while increasing too much the amount of nanoclay decreases the thermal stabilization.

Despite the exact degradation mechanism(s) is currently not clear, such a behavior is probably associated with the morphological changes in relative proportion of exfoliated and intercalated species with the clay loading. At low clay loading (e.g. 1 wt%), exfoliation dominates but the amount of exfoliated nanoclay is not enough to enhance the thermal stability through char formation [30]. When increasing the clay concentration (e.g. 2–4 wt%), much more exfoliated clay is formed, char forms more easily and effectively and consequently promotes the thermal stability of the nano-

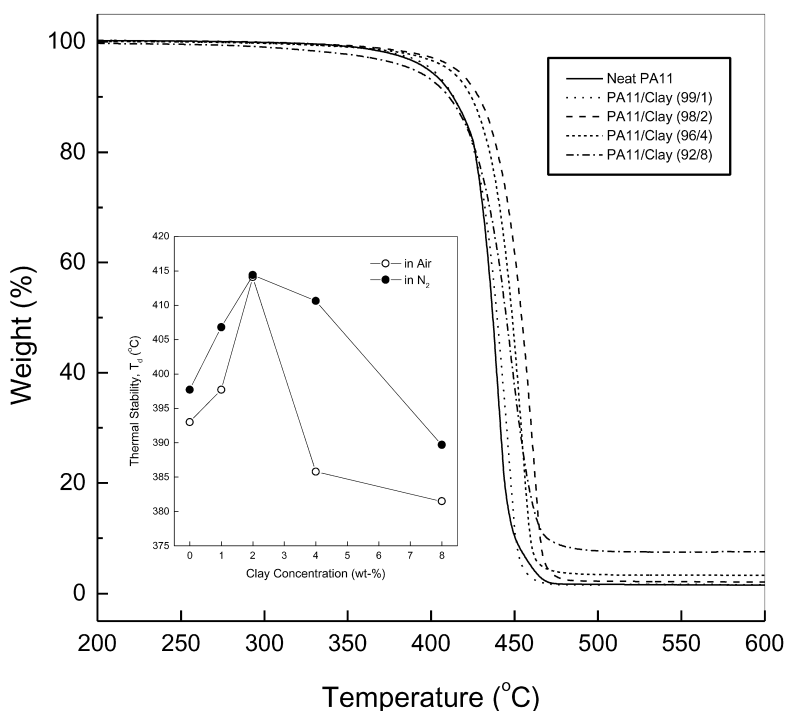


Fig. 3. Temperature dependence of weight loss for nylon 11/clay nanocomposites in nitrogen flow. The insert shows the thermal stability, characterized by decomposition temperature (T_d) in both air and nitrogen flows, as a function of clay concentration.

composites. At even higher clay loading level (e.g. up to 8 wt%), the intercalated structure is the dominant population (as evidenced by TEM in Fig. 2) and, even if char is formed in high quantity, the morphology of the nanocomposite probably does not allow for maintaining a good thermal stability. However, it is known that the chemical nature of the studied polymers and the type of clay used (such as surface modification, CEC) play an important role in their degradation behavior. Thus, care should be taken when generalizing such an explanation in nylon 11 to other polymer systems, as observed in poly(etherimide)/clay nanocomposites where intercalated nanolayers were found to be better thermal stabilizers than the exfoliated ones [31].

Fig. 4 summarizes the DMA data (Fig. 4(a)) in which the dynamic storage modulus (E') at 25 °C (ambient temperature) and the glass transition temperature (T_g), are presented as a function of clay concentration (Fig. 4(b)). It can be seen that with increasing clay loading, the storage moduli of the nanocomposites increase abruptly (up to 4 wt% of clay content), as commonly observed in other exfoliated polymer/clay systems. After that (from 4 to 8 wt%), the modulus only slightly increases with a decreasing slope (typically for the intercalated systems). The storage modulus for the nanocomposite containing 8 wt% exhibits an almost 100% increment compared with neat nylon 11. The significant improvement in storage modulus of nylon 11/clay nanocomposites is most probably ascribed to the stiff nature of clay filler (whose stiffness is considerably higher than that of PA11 matrix), and also to the combined effect of aspect ratio and degree of dispersion of clay particles. And clearly, the fine and nanoscale dispersion of organoclay plays the major role in improvement of modulus, as illustrated here. Another interesting feature from DMA is that the glass transition temperature T_g (α -relaxation) decreases steadily by about 12 °C as the clay concentration increases to 8 wt%. This decrease of T_g is probably due to the plasticizing effect from the organic modifier (surfactant) within the organically modified clay (organoclay) used in this study as the organic loading is up to about 30 wt% from the TGA data (not shown here).

Additionally, the T_g values by DMA are considerably higher than those (about 40 °C) of nylon 11 by DSC reported in Ref. [32]. In fact, as reported in many other polymeric systems, the T_g by DSC is usually about 10–15 °C lower than that by DMA. This is probably due to the following reasons: (1) The peak maximum of the $\tan\delta$ curve (usually regarded as T_g) is the center of the relaxation, whereas in the DSC experiment the onset temperature of the T_g relaxation is usually reported. In such a case, the T_g by DSC will be lower than that by DMA by an amount that varies with the specific polymer [33]; (2) In addition, there is a frequency effect which puts the mechanical (~ 1 Hz here) T_g about 17 °C higher than that for a DSC measurement (~ 0.0001 Hz) for an assumed activation energy of 400 kJ/mol (typical for polymer T_g) [33]; (3) The possible effect of

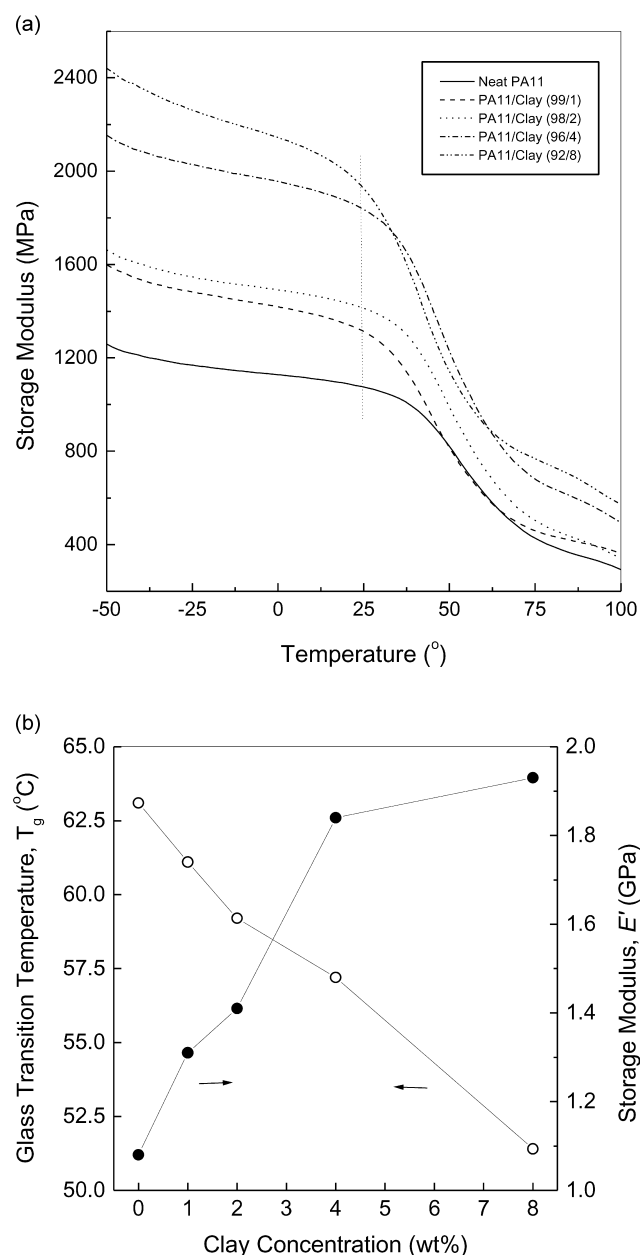


Fig. 4. (a) Storage modulus versus temperature curves; (b) glass transition temperature (T_g) and the storage modulus (E') for PA11/clay nanocomposites as a function of clay concentration.

heating rate. Here, 3 °C/min is used for DMA, and 10–20 °C/min is usually used in DSC measurements.

3.3. Tensile properties

Typical stress–strain curves for neat PA11 and PA11/clay nanocomposites are shown in Fig. 5. For neat PA11, only the curve just slightly passing the yield point is presented here. It can be seen that as clay concentration increases, an abrupt upturn in the Young's modulus is observed mainly at lower clay loadings (below 4 wt%) and eventually increases by ca. 100% up to 8 wt%, which are

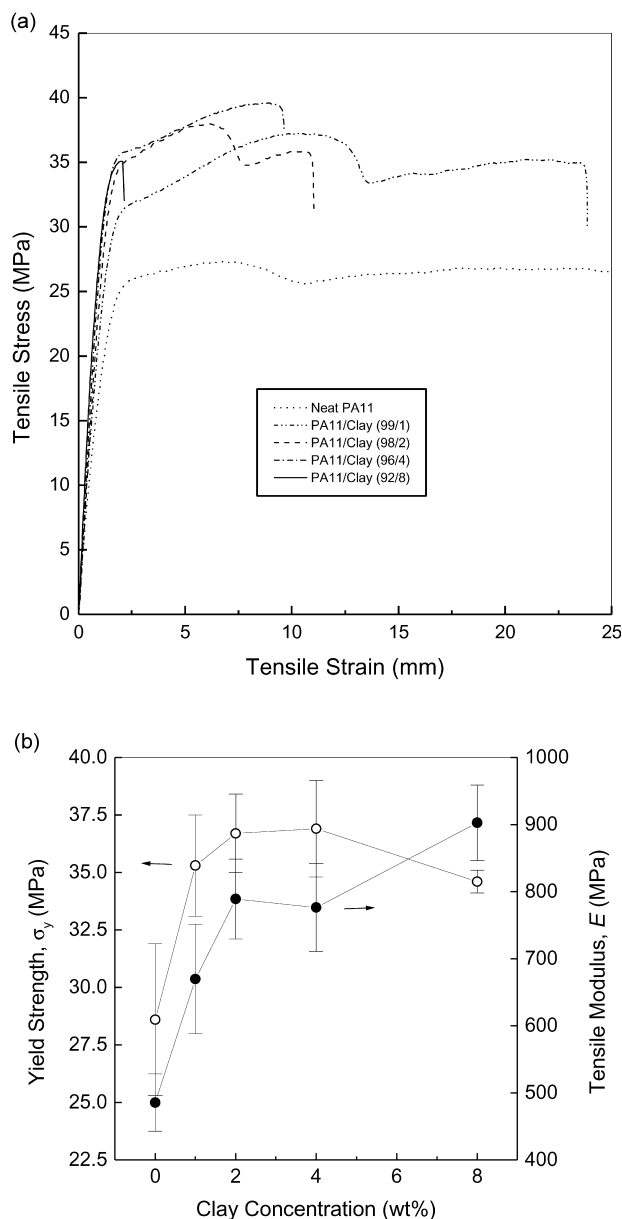


Fig. 5. (a) Stress–strain curves for nylon 11 and its clay nanocomposites at a crosshead speed of 5 mm/min; (b) tensile modulus (E) and yield strength (σ_y) of PA11/clay nanocomposites as a function of clay concentration.

consistent with the DMA results described above. Also, the yield strength of PA11/clay nanocomposites increases significantly at lower clay contents, and slightly decreases for clay concentration of 8 wt%. On the other hand, the strain at break steadily decreases with clay content, indicating that the nanocomposites become more brittle compared with neat PA11 (which breaks at about 285% of elongation). The nanocomposites containing both 1 and 2 wt% clay show a much more pronounced yield and post-yield drop than neat nylon 11. The value of tensile stress at the yield point increases with increasing the clay content as well as the elastic modulus. Also, both yield strength and modulus are considerably lower than the values reported in Ref. [32], probably due to compression molding. Generally,

the tensile testing indicates that (1) the mechanical properties of PA11/clay nanocomposites are substantially superior to those of neat PA11 due to the reinforcement of the high aspect ratio clay platelets, (2) the exfoliated nanocomposites have better improved properties than the intercalated ones due to finer dispersion of nanoclay among polymeric matrix.

4. Conclusions

A series of nylon 11/organoclay nanocomposites with different clay loadings has been prepared by melt-compounding using twin-screw extruder. XRD and TEM show the exfoliated nanocomposites are formed at low clay concentrations (less than 4 wt%) and a mixture of exfoliated and intercalated nanocomposites is obtained at higher clay contents. TGA shows that the thermal stability of the nanocomposites is improved by about 20 °C when the clay loading is lower than 4 wt%. However, the stabilization significantly decreases at higher clay concentrations probably owing to relatively poor clay dispersion. DMA shows that the storage modulus dramatically increases by about 100% when clay content is up to 8 wt% in comparison to neat nylon 11, while the glass transition temperature steadily decreases (by more than 10 °C) as a function of clay loading probably due to a plasticizing effect from the presence of organic surfactants within organoclay. The tensile tests indicate that the elastic modulus and yield strength of nylon 11/organoclay nanocomposites are significantly enhanced compared with neat nylon 11. The thermal stability and mechanical properties of the exfoliated nylon 11/clay nanocomposites (containing lower clay concentrations) are superior to those of the intercalated ones (with higher clay contents), due to the finer dispersion of organoclay among the polymer matrix. In general, the degree of dispersion of nanoclay within polymer matrix plays a vital role in property improvement. The investigations on thermal degradation mechanism and influence of nanoclay on crystalline morphology and deformation behavior of nylon 11 are still in progress.

Acknowledgements

This work is financially supported by Institute of Materials Research and Engineering (IMRE). K.P. Lim would like to appreciate the support from Professional Placement Program of Department of Materials Science, National University of Singapore.

References

- [1] Giannelis EP. Appl Organomet Chem 1998;12:675.
- [2] LeBaron PC, Wang Z, Pinnavaia TJ. Appl Clay Sci 1999;15:11.
- [3] Gilman JW. Appl Clay Sci 1999;15:31.

- [4] Porter D, Metcalfe E, Thomas MJK. *Fire Mater* 2000;24:45.
- [5] Pinnavaia TJ, Beal GW. *Polymer-clay nanocomposites*. New York: Chichester Wiley; 2000.
- [6] Heinemann J, Reichert P, Thomann R, Mulhaupt R. *Macromol Rapid Commun* 1999;20:423.
- [7] Kojima Y, Usuki A, Kawasumi M, Okada A, Kurauchi T, Kamigaito O. *J Polym Sci Polym Chem* 1993;31:983.
- [8] Usuki A, Kawasumi M, Kojima Y, Okada A, Kurauchi T, Kamigaito O. *J Mater Res* 1993;8:1174.
- [9] Usuki A, Kojima Y, Kawasumi M, Okada A, Fukushima Y, Kurauchi T, Kamigaito O. *J Mater Res* 1993;8:1179.
- [10] Kojima Y, Usuki A, Kawasumi M, Okada A, Fukushima Y, Kurauchi T, Kamigaito O. *J Mater Res* 1993;8:1185.
- [11] Cho JW, Paul DR. *Polymer* 2001;42:1083.
- [12] Fornes TD, Yoon PJ, Keskkula H, Paul DR. *Polymer* 2001;42:9929.
- [13] Fornes TD, Yoon PJ, Hunter DL, Keskkula H, Paul DR. *Polymer* 2002;43:5915.
- [14] Lincoln DM, Vaia RA, Wang ZG, Hsiao BS. *Polymer* 2001;42:1621.
- [15] Medellin-Rodriguez FJ, Burger C, Hsiao BS, Chu B, Vaia RA, Phillips S. *Polymer* 2001;42:9015.
- [16] Lincoln DM, Vaia RA, Wang ZG, Hsiao BS, Krishnamoorti S. *Polymer* 2001;42:9975.
- [17] Liu X, Wu Q. *Eur Polym J* 2002;38:1383.
- [18] Liu X, Wu Q. *Polymer* 2002;43:1933.
- [19] Dabrowski F, Bourbigot S, Delobel R, Le Bras M. *Eur Polym J* 2000;36:273.
- [20] Krishnamoorti R, Yurekli K. *Curr Opinion in Colloid Interface Sci* 2001;6:464.
- [21] Takase Y, Lee JW, Scheinbeim JI, Newman BA. *Macromolecules* 1991;24:6644.
- [22] Scheinbeim JI, Lee JW, Newman BA. *Macromolecules* 1992;25:3729.
- [23] Zhang QX, Mo ZS, Zhang HF, Liu SY, Cheng SZD. *Polymer* 2001;42:5543.
- [24] Kuchta FD, Lemstra PJ, Keller A, Baterburg LF, Fischer HR. *Mat Res Soc Symp Proc* 2000;628:CC11121.
- [25] Kojima Y, Usuki A, Kawasumi M, Okada A, Kurauchi T, Kamigaito O. *J Polym Sci Polym Chem* 1993;31:1755.
- [26] KICKELBICK G. *Prog Polym Sci* 2003;28:83.
- [27] Lepoittevin B, Pantoustier N, Devalckenaere M, Alexandre M, Kubies D, Calberg C, Jerome R, Dubois P. *Macromolecules* 2002;35:8385.
- [28] Giannelis EP. *Adv Mater* 1996;8:29.
- [29] Lagaly G. *Appl Clay Sci* 1999;15:1.
- [30] Alexandre M, Dubois P. *Mater Sci Eng* 2000;28:1.
- [31] Lee J, Takekoshi T, Giannelis EP. *Mater Res Soc Symp Proc* 1997;457:513.
- [32] Jolly L, Tidu A, Heizmann JJ, Bolle B. *Polymer* 2002;43:6839.
- [33] Cheremisinoff NP. *Elastomer technology handbook*. Boca Raton: CRC Press; 1993.